Carbohydrate Polymers 80 (2010) 555–562

Contents lists available at ScienceDirect

Carbohydrate Polymers

journal homepage: www.elsevier.com/locate/carbpol

Study on the sol–gel transition of xyloglucan hydrogels

Amanda K. Andriola Silva Brun-Graeppi [a,b], Cyrille Richard [c,d,e,f], Michel Bessodes [c,d,e,f], Daniel Scherman [b,c,d,e,f], Tetsuharu Narita [g], Guylaine Ducouret [g], Otto-Wilhelm Merten [b,*]

[a] Université d'Évry Val d'Essonne, École doctorale des Génomes Aux Organismes, Boulevard François Mitterrand, 91025 Evry cedex, France
[b] Genethon, 1 bis rue de l'Internationale, BP 60, 91002 Evry cedex, France
[c] Unité de Pharmacologie Chimique et Génétique, CNRS, UMR 8151, Paris, F-75270 cedex, France
[d] Inserm, U640, Paris, F-75270 cedex, France
[e] Université Paris Descartes, Faculté des Sciences Pharmaceutiques et Biologiques, Paris, F-75270 cedex, France
[f] ENSCP, Paris, F-75231 cedex, France
[g] Physico-chimie des Polymères et des Milieux Dispersés, UMR 7615, UPMC-CNRS-ESPCI, 10 rue Vauquelin, 75231 Paris cedex 05, France

ARTICLE INFO

Article history:
Received 13 October 2009
Received in revised form 11 December 2009
Accepted 15 December 2009
Available online 22 December 2009

Keywords:
Xyloglucan
Gelation
Thermoresponsive hydrogels
Rheology

ABSTRACT

Partially degalactosylated xyloglucan is a temperature-responsive polymer very promising for biotechnological purposes. We have studied the sol–gel transition of xyloglucan hydrogels with different galactose removal ratios. Rheological analysis was carried out, and the sol–gel transition temperature was determined at the cross-over point of G' and G''. As a general trend, the sol–gel transition temperature was reduced as the galactose removal ratio increased, and at higher polymer concentrations. The reversible gelation was studied, and a thermal hysteresis was for the first time observed and discussed. The intrinsic viscosity $[\eta]$ values of the samples and the molar mass decreased with increasing galactose removal. Light scattering analysis demonstrated that the increase in the hydrophobic content by galactose removal induced an increase in polymer–polymer interactions and a change in the molecule conformation to a more compact structure.

1. Introduction

Hydrogels are three-dimensional, cross-linked networks of water-soluble polymers. Hydrogels can be made from virtually any water-soluble polymer, encompassing a wide range of chemical compositions and bulk physical properties (Hoare & Kohane, 2008). Some hydrogels undergo continuous or discontinuous changes in swelling, which are mediated by external stimuli such as changes in pH, temperature, ionic strength, solvent type, electric and magnetic fields, light, and the presence of chelating species (Kopecek, 2007).

Temperature is the most widely used stimulus in environmentally responsive polymer systems. The change of temperature is not only relatively easy to control, but also easily applicable both *in vitro* and *in vivo* (Gil & Hudson, 2004). Temperature-responsive polymers and hydrogels exhibit a volume phase transition at a certain temperature as a consequence of a sudden change in the solvation state (Schmaljohann, 2006).

Partially degalactosylated xyloglucan is an example of temperature-responsive polymer. The native polysaccharide has a backbone consisting of glucose residues, with side groups of xylose attached through glycosidic linkage. Certain xylose residues are additionally substituted with galactose or the disaccharide galactose-fucose (Christiernin, Ohlsson, Berglund, & Henriksson, 2005; Reiter, 2002) (Fig. 1).

Xyloglucan can be rendered thermally responsive by using fungal β-galactosidase in order to remove more than 35% of the galactose residue. For treated xyloglucan, a lower and upper transition temperature from sol–gel and gel–sol, respectively, were found, and the gel was shown to be thermo-reversible upon cooling. It was also determined that with a higher galactose removal ratio (GRR) there was an increase in temperature range of the gelation peaks, hence a broader gelation range (Shirakawa, Yamatoya, & Nishinari, 1998).

Xyloglucan gel is obtained from solutions whose concentration are usually 1–2% (Miyazaki et al., 1998), but strong hydrogels were only obtained at 3 wt.% at 37 °C (Nisbet et al., 2006). The gelation process is believed to result from hydrophobic interactions (Miyoshi, Takaya, & Nishinari, 1996). Microstructural and rheological results indicated that the gelation of xyloglucan occurs as a two-stage process. The first step, which is not concentration dependent, is the initial formation of large membrane structures in the pre-gel. This accounts for the initially high modulus. The formation of the membrane structures appears to be accelerated by the presence of ions in the phosphate buffer. The second stage involves the joining of membranes into a very strong 3-dimensional network. This

* Corresponding author. Tel.: +33 (0) 1 69 47 25 90; fax: +33 (0) 1 60 77 86 98.
E-mail address: omerten@genethon.fr (O.-W. Merten).
URL: http://www.genethon.fr (O.-W. Merten).

0144-8617/$ - see front matter © 2009 Elsevier Ltd. All rights reserved.
doi:10.1016/j.carbpol.2009.12.026

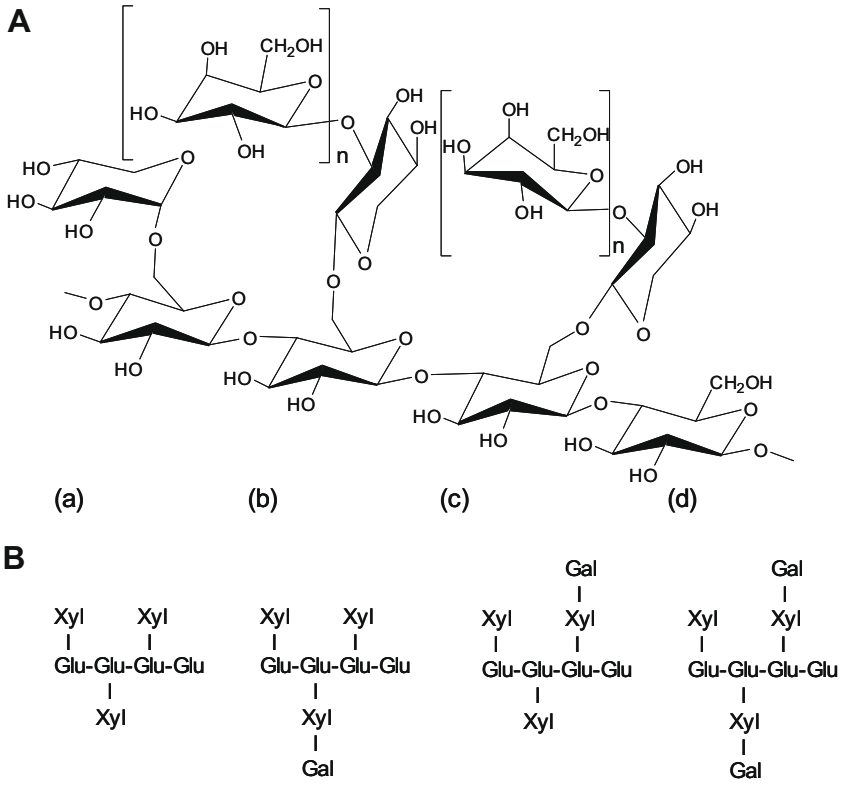

Fig. 1. Structure of xyloglucan. (A) The structure of the repeating units of xyloglucan. (B) The unit structures of oligosaccharides from tamarind xyloglucan showing (a) heptasaccharide, (b and c) octasaccharide, and (d) nonsaccharides (Nanjawade, Manvi, & Manjappa, 2007).

process and the final morphology are independent of the solution media (Nisbet et al., 2006).

Considering the properties of xyloglucan, this polymer may be very promising for biotechnological purposes. However, there are very few data on the rheological and structural characteristics of these hydrogels (Klouda & Mikos, 2008). The most recent work on this hydrogel is limited to xyloglucan with a 48% galactose removal ratio (Nisbet et al., 2006). Another study, concerning the gelation of xyloglucan with different galactose removal ratios as a function of the temperature, is mainly based on the visual observation of gelation and only some rheological data have been provided (Shirakawa et al., 1998). The aim of the present work was to provide further physico-chemical evaluation of the sol–gel transition of xyloglucan hydrogels with different galactose removal ratios. Rheology analysis was carried out. Molar mass determination and dynamic and static light scattering analyses were performed to evaluate the correlation between galactose removal ratio, molar mass, polymer–polymer interaction and molecular conformation.

2. Materials and methods

Xyloglucan from *Tamarindus indica* was obtained from Megazyme International Ireland Ltd. (Ireland). β-Galactosidase from *Aspergillus oryzae* (11.8 U/mg) was purchased from Sigma Chemicals (USA). The galactose removal ratio was determined using an enzymatic kit, Lactose/D-Galactose UV method for enzymatic analysis, Roche/r-Biopharm (Germany).

2.1. β-Galactosidase reaction

The production of xyloglucan with different GRR was carried out by reacting a 2% aqueous solution of xyloglucan with the enzyme β-galactosidase from *A. oryzae* at 7.4 U/mL. The reaction was carried out at pH 5.0 and 50 °C. Samples were taken at different intervals 8, 16, 24 and 32 h. They were identified as T8, T16, T24 and T32, respectively (T0 corresponded to the native polymer). The samples were then heated at 100 °C for 20 min to inactivate the enzyme. The enzyme-degraded xyloglucan was precipitated from this solution by addition of ethanol. After three cycles of redispersion in water/precipitation in ethanol for purification, the product was dried at 60 °C during two days. The supernatant obtained during purification was analyzed for its galactose content using an enzymatic kit, Lactose/D-Galactose UV method. The GRR was determined as:

$$\text{GRR} = \text{Released galactose residues} \times 100/\text{total galactose residue} \quad (1)$$

The amount of total galactose residues was measured after total hydrolysis by heating the polymer with 2 N sulfuric acid at 100 °C for 3 h (Shirakawa et al., 1998).

Sample solutions were prepared by dissolving the appropriate amount of purified xyloglucan powder in phosphate buffer (PBS) and stirring at 4 °C for two days. The obtained solutions were stored at 4 °C.

2.2. Rheology

The thermogelation properties of xyloglucan was evaluated by rheology. The oscillatory shear measurements were performed on a stress controlled rheometer RS600 Haake (Germany) equipped with a cone-and-plate geometry (35 mm diameter, 2° angle and gap size of 103 μm). The values of the stress amplitude were checked to ensure that all measurements were conducted within the linear viscoelastic regime, where the dynamic storage modulus (G') and loss modulus (G'') are independent of the stress amplitude. The measuring unit was equipped with a temperature unit (Peltier

plate) that provided temperature control during analysis. Rheological behavior of the sol–gel transition was measured by performing temperature sweeps. Temperature dependence of storage (G') and loss (G'') moduli were observed by heating the systems from 10 to 60 °C at a rate of 0.5 °C/min. The samples were protected by a homemade cover to prevent water evaporation.

2.3. Viscometry

Capillary viscometry for xyloglucan samples was performed at 25 °C with a Ubbelohde Viscometer (Schott Instruments, Germany) in order to determine the intrinsic viscosity [η] at 25 °C of polymer solutions in water.

Molar mass (M) was evaluated from the intrinsic viscosity measurements using the Mark–Houwink equation:

$$[\eta] = KM^a$$

where [η] is the intrinsic viscosity in dL/g, K and a are constants whose values depend on the nature of the polymer, the temperature and of the solvent. For this study, we considered $[\eta] = 8 \times 10^{-4}$ $M^{0.66}$, based on data from the literature (Picout, Ross-Murphy, Errington, & Harding, 2003).

Viscometric measurements of dilute and semi-dilute solutions were performed for T0 and T24 using a Contraves Low-Shear 30 Viscometer. For all the experiments, the temperature was fixed at 25 °C. The critical overlapping c^* values were obtained from the linear variation of the viscosity as a function of the polymer concentration.

2.4. Size-exclusion chromatography

The molar mass and the intrinsic viscosity of xyloglucan samples were also evaluated by size-exclusion chromatography (SEC). The chromatography system was equipped with Shodex OH-Pack SB-804 HQ and SB-805 HQ Shodex OH SB-G columns connected in series with a pre-column Shodex OH SB-G (Shodex, Showa Denko KK, Japan). The refractive index (RI) signal was measured using an ERC-7517A RI detector. A Viscotek 270 dual detector was used for low and right angle light scattering and viscosity (Viscotek, USA). The mobile phase was an aqueous solution of $NaNO_3$ 50 mM + NaN_3 0.02% delivered at a flow rate of 0.7 mL min^{-1}, with an injection volume of 50 μL. Dextran and pullulan standards with molar mass of 65 and 150 kDa were used (Viscotek, USA). All data were acquired and analyzed using Omnisec software (Viscotek, USA).

2.5. Dynamic and static light scattering

The measurements in both static and dynamic mode were performed at 20 °C with a ALV-5000 System comprising a compact goniometer system and a multi-τ real-time digital correlator (ALV−Laser Vertriebsgesellschaft m.b.H., Langen, Germany). The angular range applied was from 30° to 150° in steps of 10°. The duration of single measurements was typically 10 s averaged over 3 runs (ALV/Static & Dynamic Fit and Plot Program used). A He−Ne laser (λ_0 = 632.8 nm) was the light source, and the scattering of toluene was used as the primary standard. The refractive index increment, dn/dc, was chosen as 0.1583 mL g^{-1} (Urakawa, Mimura, & Kajuwara, 2002). Solutions used for light scattering were solutions of 0.05% polymer and serial dilutions (0.03%, 0.02%, and 0.01%). These solutions were filtered directly into the cylindrical light scattering cuvettes (Pyrex disposable culture tubes, Corning Incorporated, Corning, New York) using Particulate Filter Unit Millex®-AA 0.8 μm syringe filters (Millipore).

3. Results and discussion

3.1. β-Galactosidase reaction

In order to render xyloglucan thermoresponsive, the galactose side-chains were partially removed from the native xyloglucan from *T. indica* using β-galactosidase. The GRR as a function of the reaction time is presented in Fig. 2. The reaction protocol was the same used by Shirakawa et al. (1998), but xyloglucan from another supplier was evaluated. According to the results from Shirakawa et al. (1998), the expected values would be near 30%, 40% and 48% for T8, T16 and T24, respectively. The corresponding GRR for 32 h of reaction is not shown. Concerning our results, T8, T16, T24 and T32 presented a GRR of 21%, 30%, 40% and 85%, respectively. The observed variation may be ascribed to the origin of the polymer and to the galactose dosage method. The data reported here have been obtained by using an UV method for enzymatic analysis for Megazyme xyloglucan, while Shirakawa's results were obtained from a HPLC determination for Dainippon Sumitomo Pharma xyloglucan.

3.2. Rheology

Dynamic rheology is one of the most extensive methods to study rheological properties of polysaccharide gel, and is also the most direct and reliable way for the determination of the sol–gel transition (Zhang, Xu, & Zhang, 2008).

In this study, sol–gel transition evaluation was based on the temperature of G' and G'' cross-over (Chauvelon, Doublier, Buléon, Thibault, & Saulnier, 2003; Dai, Liu, Liu, & Tong, 2008; Li, Lim, Wang, & Jiang, 2008; Miyoshi et al., 1996; Ruan, Lue, & Zhang, 2008). The effect of temperature on the dynamic moduli (G' and G'') for xyloglucan samples at different GRR and at a total polymer concentration of 2 wt.% in PBS is depicted in Fig. 3.

For all the temperature range, the T0, T8 samples remained in the sol state, as indicated by $G'' > G'$. The values of the storage and the loss moduli are typical of low viscous systems with a low degree of elasticity. At higher GRR, the samples presented a different behavior. T16, T24 and T32 had their transition temperature at about 55, 43 and 37 °C, respectively. No plateau of G' was reached for T16, T24 and T32. Probably, this is related to the temperature range limited to 60 °C and to the slow gel formation process. For some polysaccharides, we observed that an initial rise in modulus followed the establishment of a three-dimensional network structure and involved the conversion of increasing amounts of chains in the sol fraction into the gel. Subsequently, there was only a slower rise in modulus. The transition from the stage of rapidly increasing modulus to the pseudoplateau stage presumably occurs when most (or virtually all) of the sol fraction has been converted into the gel phase (Clark, Gidley, Richardson, & Ross-Mur-

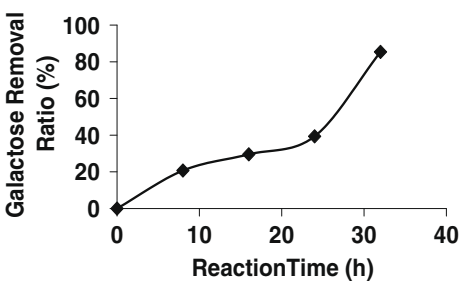

Fig. 2. Galactose removal ratios as a function of the reaction time for xyloglucan samples.

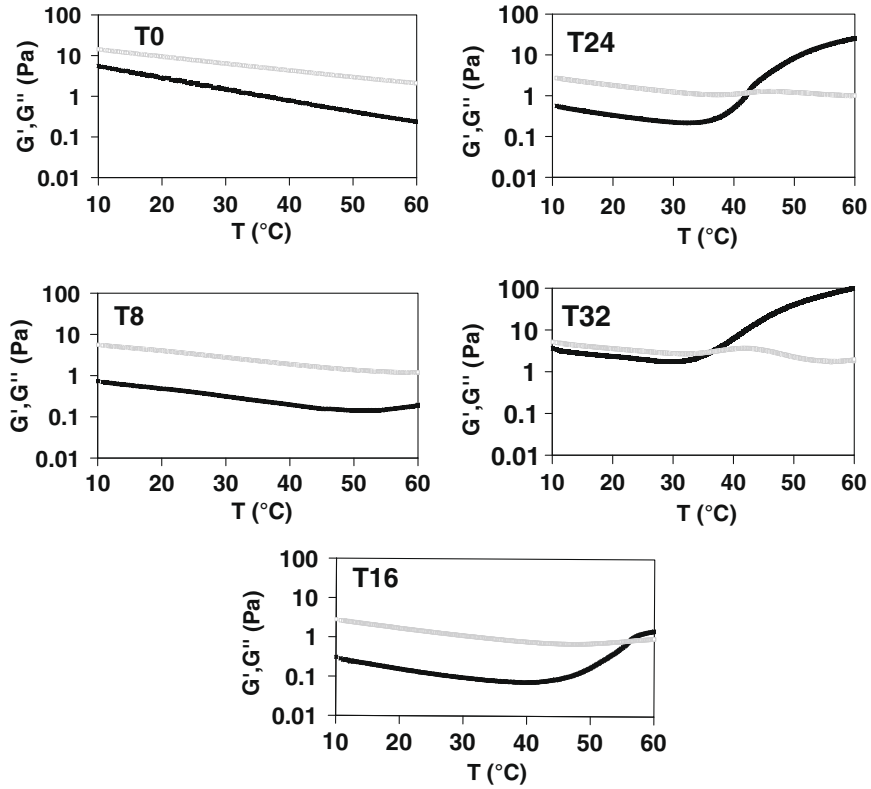

Fig. 3. Temperature dependence on the dynamic moduli – G' (black) and G'' (grey) – for xyloglucan samples.

phy, 1989). Therefore, for T16, T24 and T32 at 60 °C, the gelation process was not complete.

Although T16, T24 and T32 are both considered as gel at 60 °C, for instance, their strength is quite different according to their tan δ (G''/G') value (Fig. 4). For a conventional elastic gel, tan δ < 0.1 (Ikeda & Nishinari, 2001), this is the case of T24 and T32. T16 can be considered as a typical weak gel, with a tan δ > 0.1 (Ikeda & Nishinari, 2001). Except for T16, the other products present a tan δ value that can be compared to other biopolymer gels such as gelatin and agarose, whose tan δ values vary from 0.03 to 0.07 (Chronakis, Piculell, & Borgström, 1996).

As a general trend, tan δ decreased as the temperature rose from 10 to 60 °C. The sol–gel transition temperature was reduced as galactose removal ratio increased. At low values of galactose removal, there is a steric hindrance that renders difficult main chain interaction to form a gel, while at higher values this interaction is strong enough to build up a network (Shirakawa et al., 1998).

In fact, xyloglucan presents hydrophobic segments (main chain) coupled to hydrophilic ones (galactose moieties). These kinds of molecules are water soluble at low temperature and as the temperature increases, hydrophobic domains aggregate to minimize the hydrophobic surface area contacting the bulk water, thus reducing the amount of structured water surrounding the hydrophobic domains and maximizing the solvent entropy. The temperature at which gelation occurs depends on the concentration of the polymer, the length of the hydrophobic segment, and the chemical structure of the polymer: the more hydrophobic the segment, the larger the entropic cost of water structuring, the larger the driving force for hydrophobic aggregation, and the lower the gelation temperature (Hoare & Kohane, 2008). This is observed as GRR increases.

In order to investigate gel–sol transition as well, a cooling cycle was performed for T24 after the heating cycle (Fig. 5). As temperature increased, G' presented a slight drop until about 35 °C and showed superior values onwards. G'' presented a different profile. The evolution of such modulus during heating cycle showed three different regions. Its value decreased, increased slightly after 40 °C and then decreased again after around 45 °C. The viscosity decreased smoothly between 10 and 30 °C following Arrhenius behavior characterized by an activation energy around E_a = 32 kJ/mol. This value is rather close to the activation energy for polymer solutions. Moreover, E_a is the same before and after the enzymatic treatment. The same behavior has been described for thermo-

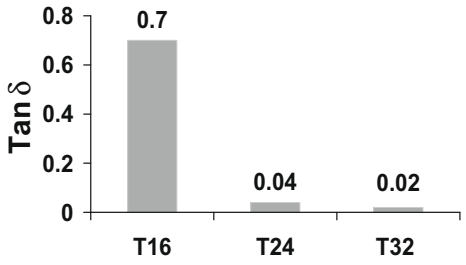

Fig. 4. tan δ values for T16, T24 and T32 at 60 °C.

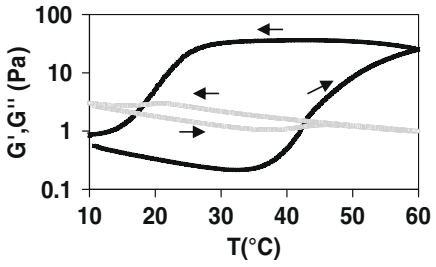

Fig. 5. Temperature dependence on the dynamic moduli – G' (black) and G'' (grey) – for T24 xyloglucan during heating (→) and cooling cycles (←).

responsive polymers and its backbone. At near 43 °C, at a heating rate of 0.5 °C/min, G' and G'' crossed, but as the gel passed to higher temperatures, G' assumed much higher values than G'' and the sample became a gel.

For the cooling cycle, G' remained superior to G'' even if the temperature was about 25 °C. G' decrease took place in two steps. The first one may be caused by the melting of weaker junction zones of non-aggregated chains while the second step decrease in G' may have been induced by the melting of stronger junction zones formed by the aggregated chains. This observation was characteristically similar to those of gellan gel and agar/k-carrageenan (Norziah, Foo, & Karim, 2006).

The gradual decrease in G' with temperature in the cooling process showed an outstanding deviation from the heating curve. This behavior clearly indicates a hysteresis, as heating and cooling curves do not overlap. For a thermoresponsive gel whose cooling path does not follow the same trace as that in the heating process, such as shown in Fig. 5, there is a higher critical gelation temperature on heating and a lower temperature on cooling (Li et al., 2001). Such behavior is also observed for other polysaccarides as κ-carrageenan (Chronakis et al., 1996; Núñez-Santiago & Tecante, 2007; Wang, Rademacher, Sedlmeyer, & Kulozik, 2005), schizophyllan-sorbitol (Yapeng Fang, 2004), agarose (Mohammed, Hember, Richardson, & Morris, 1998), cellulose (Ruan et al., 2008) and methylcellulose (Li et al., 2001) and depends on the heating/cooling rate.

The impact of the cooling/heating rates on the transition temperature of the samples is related to the chain association dynamics. If we consider a slow heating rate, the sol–gel transition will take place at a reduced temperature compared to the transition temperature observed in a fast heating rate. This is because the polymer chains are given a reduced time extent to associate when they undergo a fast heating rate. In the same way, the gel–sol transition during the cooling phase will take place in a superior temperature for a slow cooling rate.

The thermal hysteresis in a thermoreversible gel is often caused by the aggregation of rigid polymer chains (Yapeng Fang, 2004) and the existence of some associated aggregates or weak connections that have not been completely disassociated (Li et al., 2001). The outstanding difference in the critical gelation temperature between the heating and cooling processes is due to the kinetics of association and dissociation, or in other words to nonequilibrium conditions. Another factor that may affect the dissociation is the time for which the system has equilibrated at the highest temperature before starting the cooling process. In this work, the cooling process was initiated immediately, as soon as the highest temperature had been reached in the heating process. However, if the sample is allowed to equilibrate for some time before cooling, the time should have a significant effect on the dissociation behavior in the following cooling process, and this effect should be dependent on the time need to reach the gelation equilibrium. When the gel system has developed near to its equilibrium state at the given temperature, the sample should be more difficult to dissociate in the cooling process, because of the perfect network formed, compared to a freshly formed gel at the same temperature. On the other hand, when the sample is far from the equilibrium state, the dissociation should be easier, resulting in a lower critical sol–gel transition. Therefore, the gelation in a heating process can be different from that under isothermal conditions because of the nonequilibrium conditions existing during a kinetic process (Li et al., 2001).

For xyloglucan hydrogels, the time effect on G' and G'' was studied. Fig. 6 illustrates the change with time of dynamic moduli for 2% T24 at 60 °C. For these parameters, a linear increase was observed and no plateau was reached until 1200 s. The same phenomenon has also been observed for other polysaccharides, in which the time for moduli to reach their equilibrium values has been reported to be up to 15 h, with a ratio between the final and the initial G' of at least two (Tecante & Doublier, 1999).

In the range from 10 to 60 °C, we observed that the sol–gel transition temperature significantly shifts to lower temperatures when the polymer concentration increased.

Fig. 7 shows the temperature dependence of G' and G'' curves for T24 xyloglucan solutions at 1.5, 2 and 2.5 wt.%. Regarding 1.5 wt.% solution, G' curve crossed over G'' one at about 40 °C. It should be noted that G' reached the lowest value at 30 °C before the cross-over point, and then gradually increased. The increase of G' was a result of the partial formation of xyloglucan interactions through its self-association in solution. Subsequently, both G' and G'' increased gradually, but G' exhibited a much higher increasing rate than that of G''. This suggests that elevation of the temperature mainly induced the increase in elasticity of the system, and the formation of an elastic gel network. The G' and G'' curves at 2 and 2.5 wt.% xyloglucan solution showed a similar pattern. However, the distance between the point G' started to increase and the cross-point of G' and G'' appeared to shorten as the concentration

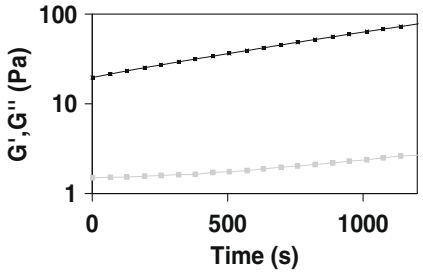

Fig. 6. Time evolution of dynamic moduli – G' (black) and G'' (grey) – for 2% T24 at 60 °C.

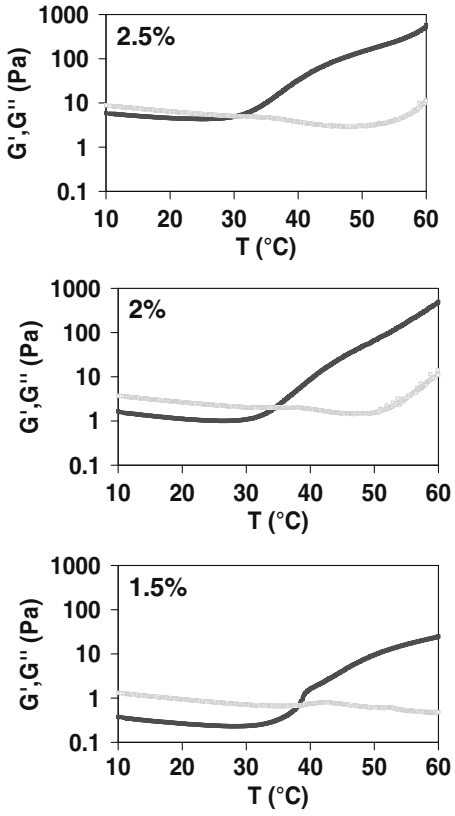

Fig. 7. G' (black) and G'' (grey) dependence on the concentration of the polymer for T24 xyloglucan samples at 1.5, 2 and 2.5 wt.%.

increased. Besides, the sol–gel transition temperature decreased with an increase of the polymer concentration. This suggests that the aggregation and entanglements of the polymer chains can be caused not only by heating but also by elevated concentration. The reason for this could be the fact that the elevation of the polymer concentration favors polymer collisions, promoting the formation of the gel network. At lower concentration, higher temperature is needed to establish the interactions necessary to form the gel network (Ruan et al., 2008; Weng, Zhang, Ruan, Shi, & Xu, 2004).

Interestingly, the curves for this T24 at 2% did not fit the one presented above (Fig. 3, T24). Both samples were similar, but this one underwent stirring for 48 h before measurement, while the one first presented (Fig. 3, T24) was allowed to rest for one week before measurements. This is not surprising as it is well known for other polysaccharides that standing and stirring may have an effect on gelation (Chauvelon et al., 2003; Michon, Chapuis, Langendorff, Boulenguer, & Cuvelier, 2004, 2005).

3.3. Viscometry

For all samples, the reduced viscosity was plotted against concentration. The intrinsic viscosity was obtained by the extrapolation of the reduced viscosity to zero polymer concentration. Molar mass (M) was evaluated from the intrinsic viscosity measurements. The results are summarized in Table 1.

The intrinsic viscosity [η] appeared to be at the same order of magnitude for the different samples. As expected, the [η] values of the samples increased with increasing molar mass and varied from about 4.1 to 7.5 dL/g for xyloglucan samples with molar mass ranging from 418×10^3 to 1040×10^3 g/mol. The same trend is also observed for other polysaccharides such β-glucan (Lazaridou, Biliaderis, & Izydorczyk, 2003). The intrinsic viscosity, which reflects the hydrodynamic volume occupied by a molecule, is an index of the capacity of a polymer molecule to enhance the viscosity. The decrease in intrinsic viscosity means a decrease of the hydrodynamic volume of the macromolecular chain. Therefore, the values of the molar mass and the intrinsic viscosity were in agreement with the GRR of the samples, as the molecule size is expected to decrease as the GRR increases.

The solution behavior of T0 and T24 samples was examined by measuring their viscosity at various concentrations of the polysaccharide. The plot in Fig. 8 shows a pronounced increase in the viscosity above a specific critical concentration (c^*). At low polymer concentrations (dilute region), the viscosity increased approximately linearly with increasing concentration, but at higher concentrations (semi-dilute domain), the slopes changed abruptly to much higher values. This behavior is attributed to the transition from the dilute regime, where individual polymer molecules are present as isolated coils, to a semi-dilute regime where the polymer coils begin to overlap each other. Thus, c^* marks the point where the individual coils start to entangle and the onset of significant coil overlap and interpenetration (Bercea, Morariu, Ioan, Ioan, & Simionescu, 1999). The critical concentration (c^*) depends on the molar mass of the polymer. The value of c^* may progressively decrease with increasing molar mass of the polysaccharide (Lazaridou, Biliaderis, & Kontogiorgos, 2003). In our case, the critical overlapping concentration c^* value was 0.46% and 0.54%, respectively, for T0 and T24 samples.

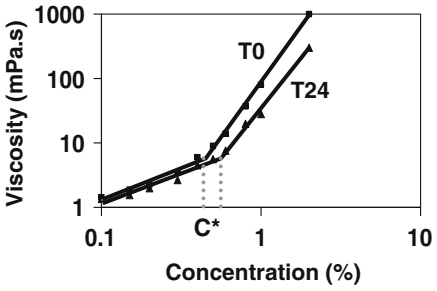

Fig. 8. Viscosity dependence on the concentration of the polymer for T24 and T0 for xyloglucan samples.

Actually, the c^* value also depends on the structure of the polymer, its chain stiffness and the flow characteristics. This can explain the slightly inferior critical overlapping concentration c^* value for the unmodified polymer T0 compared to T24 sample. In fact, more extended molecules increase the viscosity to greater extents at low concentrations than more compact molecules of similar molar mass. Therefore, stiff molecules tend to present reduced critical overlapping concentration c^* value. T0 probably exhibits a less compact structure in which hydrophobic intramolecular associations are less intense due to the galactose presence. This discussion is further addressed in the following sections.

3.4. Size-exclusion chromatography

The results concerning the intrinsic viscosity and the molar mass from capillary viscometry could be confirmed by SEC. The obtained values were quite in agreement, as shown in Table 2.

The intrinsic viscosity and the molar mass decreased as GRR increased for xyloglucan samples. Concerning the molar mass values, they concern the peak molar mass (M_p) instead of the weight averaged molar mass (M_w). T0 and T8 presented M_w values close to M_p and a single peak in the light scattering curve as a function of the retention volume. The profile of the other samples, however, was remarkably consistent with a two-population model as a new peak arose at the retention volume of 12 mL (results not shown). The intensity of this peak increased as GRR increased, and M_w values were no more in agreement with M_p ones for T16, T24 and T32 (Fig. 9). In fact, M_w might have increased as the reaction proceeded as a consequence of chain aggregation induced by the removal of hydrophilic galactose moieties and the reduced steric hindrance between the polymer molecules.

3.5. Dynamic and static light scattering

The parameters radius of gyration (R_g), hydrodynamic radius (R_h) and the second virial coefficient (A2) were obtained for xyloglucan hydrogels (Table 3). For T0, the molar mass was about

Table 1
Intrinsic viscosity and molar mass of the xyloglucan samples by capillary viscometry.

Sample	Intrinsic viscosity [η] (dL/g)	Molar mass (g/mol)
T0	7.5	1040×10^3
T8	5.3	616×10^3
T16	4.2	433×10^3
T24	4.1	418×10^3
T32	– (not reproducible)	– (not reproducible)

Table 2
Intrinsic viscosity and molar mass of the xyloglucan samples by size-exclusion chromatography.

Sample	Intrinsic viscosity [η] (dL/g)	Molar mass (g/mol)
T0	7.02	888×10^3
T8	3.88	431×10^3
T16	3.68	412×10^3
T24	3.44	353×10^3
T32	3.01	398×10^3

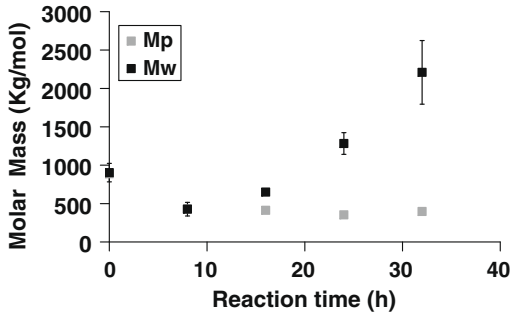

Fig. 9. Peak molar mass (M_p) and weight averaged molar mass (M_w) for xyloglucan samples as a function of the reaction time.

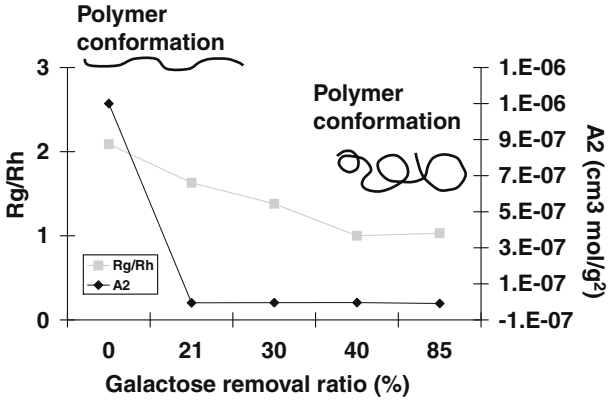

Fig. 10. Radius of gyration (R_g)/hydrodynamic radius (R_h) ratio and the second virial coefficient (A2) as a function of the galactose removal ratio for xyloglucan samples.

10^6 g/mol. This value is in agreement with our results from capillary viscometry and SEC data and literature reports (Picout et al., 2003). However, the molar mass of all samples was in the same order of magnitude, and the exact difference in molar mass between them could not be observed.

The second virial coefficient reflects solute–solute and solute–solvent interactions, and the numerical value and the sign of the coefficient indicates whether there are attractive or repulsive interactions (Murphy, 1997). For T0, A2 was positive indicating that the solution was a good polymer–solvent systems. This may be explained by the presence of the hydrophilic galactose groups. As the GRR increased, this coefficient became negative and at 25 °C the smaller value was found for T32 (Fig. 10).

Another important point is the structural parameter ρ. It can be used to ascertain whether the molecule in solution is globular, rod-like, or intermediate in shape (Murphy, 1997). Compact spherical structures present ρ of about 0.8, flexible linear chains take values of ρ from 1.2 to 1.5, but ρ of stiff polymer chains exceeds 2 (Kanao, Matsuda, & Sato, 2003). The value for this parameter was reduced as GRR increased, indicating that the molecule became more compact (Fig. 10). This is in agreement with A2 data. Such conformational change may be induced by an increase in polymer–polymer interactions due to the reduced steric hindrance resulting from the removal of hydrophilic galactose moieties. In the same way, the temperature increase influenced ρ and A2 values, indicating the induction of a slightly more compact structure.

The influence of hydrophilic/hydrophobic balance on the polymer–polymer interactions and molecule conformation has been reported in other studies. Copolymers of poly(ethoxyethyl glycidyl ether)/poly(ethylene oxide)/poly(D,L-lactide) were obtained by anionic polymerization. Light scattering analysis showed the effect of hydrophobic lactide content on A2 and on the structural parameter ρ. Like in our study, the increase in the hydrophobic content induced a reduction on the value of A2 and ρ, indicating an increase in polymer–polymer interactions and a change in the molecule conformation to a more compact structure (Dimitrov, Porjazoska, Novakov, Cvetkovska, & Tsvetanov, 2005).

In fact, the degree of hydrophobic group influence on the polymer–polymer interactions and molecule conformation depends on its content. For instance, poly(ethylene oxide)-b-poly(alkylglycidyl ether) diblock copolymers were synthesized and analyzed by light scattering. The hydrophobic blocks were formed by polymerization of alkylglycidyl ethers differing in the size of the hydrophobic portion and the length of the oxyethylene spacer between the terminal hydrophobes and the polymerizable epoxy group. A2 was not significantly influenced by the incorporation of hydrophobic groups into the copolymer macromolecule. The properties of the copolymers were very close to those of the unmodified high molecular weight poly(ethylene oxide). In this case, the negligible influence of hydrophobic groups may be related to its low content of only 2 wt.% (Petrov et al., 2002).

4. Conclusion

A sol–gel transition study for xyloglucan hydrogels with different galactose removal ratios (GRR) has been carried out. The parameter tan δ (G''/G') decreased with increasing temperature. As the temperature is increased, hydrophobic domains aggregate to minimize the hydrophobic surface area contacting the bulk water, thus reducing the amount of structured water surrounding the hydrophobic domains, and causing gelation (Hoare & Kohane, 2008). As expected, the sol–gel transition temperature decreased for higher GRR, since at low values of galactose removal, a steric hindrance renders difficult main chain interaction to form a gel. It was found that the sol–gel transition temperature was decreased for higher polymer concentration, and this may be related to the most intense polymer collision and contact. Besides, it was demonstrated for the first time that xyloglucan hydrogels present thermal hysteresis. Concerning the intrinsic viscosity [η] values and the molar mass of the samples, they decreased with increasing GRR. Light scattering analysis demonstrated that the increase in the hydrophobic content by galactose removal induced a reduction on the value of the virial coefficient A2 and the structural parameter ρ, indicating an increase in polymer–polymer interactions and a change in the molecule conformation to a more compact structure.

Table 3
Dynamic and static light scattering data for xyloglucan samples.

Sample	Temperature (°C)	A2 (10^6 cm^3 mol/g^2)	R_g (nm)	R_h (nm)	ρ (R_g/R_h)	M (g/mol)
T0	25	1.1	142	68	2.09	1.45×10^6
T0	60	−0.8	81	55	1.47	5.8×10^5
T8	25	−0.0049	83	51	1.63	4.8×10^5
T16	25	−0.0047	101	73	1.38	7.8×10^5
T24	25	−0.0039	110	110	1	1×10^6
T24	60	−0.89	100	110	0.9	1×10^6
T32	25	−0.0092	118	114	1.03	9.9×10^5

Acknowledgements

This research was supported by the grants IngeCell from Medicen Paris Region and CSCELO from the "Agence Nationale de la Recherche" – ANR05PRIB01601. We also acknowledge Dr. Ralet – UR1268, INRA, Nantes, France, for SEC analysis.

References

Bercea, M., Morariu, S., Ioan, C., Ioan, S., & Simionescu, B. C. (1999). Viscometric study of extremely dilute polyacrylonitrile solutions. *European Polymer Journal, 35*, 2019–2024.

Chauvelon, G., Doublier, J.-L., Buléon, A., Thibault, J.-F., & Saulnier, L. (2003). Rheological properties of sulfoacetate derivatives of cellulose. *Carbohydrate Research, 338*, 751–759.

Christiernin, M., Ohlsson, A. B., Berglund, T., & Henriksson, G. (2005). Lignin isolated from primary walls of hybrid aspen cell cultures indicates significant differences in lignin structure between primary and secondary cell wall. *Plant Physiology et Biochemistry, 43*, 777–785.

Chronakis, I. S., Piculell, L., & Borgström, J. (1996). Rheology of kappa-carrageenan in mixtures of sodium and cesium iodide: Two types of gels. *Carbohydrate Polymers, 31*, 215–225.

Clark, A. H., Gidley, M. J., Richardson, R. K., & Ross-Murphy, S. B. (1989). Rheological studies of aqueous amylose gels: The effect of chain length and concentration on gel modulus. *Macromolecules, 22*, 346–351.

Dai, L., Liu, X., Liu, Y., & Tong, Z. (2008). Concentration dependence of critical exponents for gelation in gellan gum aqueous solutions upon cooling. *European Polymer Journal, 44*, 4012–4019.

Dimitrov, P., Porjazoska, A., Novakov, C. P., Cvetkovska, M., & Tsvetanov, C. B. (2005). Functionalized micelles from new ABC polyglycidol–poly(ethylene oxide)–poly(D,L-lactide) terpolymers. *Polymer, 46*, 6820–6828.

Gil, E. S., & Hudson, S. M. (2004). Stimuli-responsive polymers and their bioconjugates. *Progress in Polymer Science, 29*, 1173–1222.

Hoare, T. R., & Kohane, D. S. (2008). Hydrogels in drug delivery: Progress and challenges. *Polymer, 49*, 1993–2007.

Ikeda, S., & Nishinari, K. (2001). "Weak Gel"-type rheological properties of aqueous dispersions of nonaggregated carrageenan helices. *Journal of Agricultural and Food Chemistry, 49*, 4436–4441.

Kanao, M., Matsuda, Y., & Sato, T. (2003). Characterization of polymer solutions containing a small amount of aggregates by static and dynamic light scattering. *Macromolecules, 36*, 2093–2102.

Klouda, L., & Mikos, A. G. (2008). Thermoresponsive hydrogels in biomedical applications. *European Journal of Pharmaceutics and Biopharmaceutics, 68*, 34–45.

Kopecek, J. (2007). Hydrogel biomaterials: A smart future? *Biomaterials, 28*, 5185–5192.

Lazaridou, A., Biliaderis, C. G., & Izydorczyk, M. S. (2003). Molecular size effects on rheological properties of oat [beta]-glucans in solution and gels. *Food Hydrocolloids, 17*, 693–712.

Lazaridou, A., Biliaderis, C. G., & Kontogiorgos, V. (2003). Molecular weight effects on solution rheology of pullulan and mechanical properties of its films. *Carbohydrate Polymers, 52*, 151–166.

Li, L., Lim, L. H., Wang, Q., & Jiang, S. P. (2008). Thermoreversible micellization and gelation of a blend of pluronic polymers. *Polymer, 49*, 1952–1960.

Li, L., Thangamathesvaran, P. M., Yue, C. Y., Tam, K. C., Hu, X., & Lam, Y. C. (2001). Gel network structure of methylcellulose in water. *Langmuir, 17*, 8062–8068.

Michon, C., Chapuis, C., Langendorff, V., Boulenguer, P., & Cuvelier, G. (2004). Strain-hardening properties of physical weak gels of biopolymers. *Food Hydrocolloids, 18*, 999–1005.

Michon, C., Chapuis, C., Langendorff, V., Boulenguer, P., & Cuvelier, G. (2005). Structure evolution of carrageenan/milk gels: Effect of shearing, carrageenan concentration and nu fraction on rheological behavior. *Food Hydrocolloids, 19*, 541–547.

Miyazaki, S., Suisha, F., Kawasaki, N., Shirakawa, M., Yamatoya, K., & Attwood, D. (1998). Thermally reversible xyloglucan gels as vehicles for rectal drug delivery. *Journal of Controlled Release, 56*, 75–83.

Miyoshi, E., Takaya, T., & Nishinari, K. (1996). Rheological and thermal studies of gel–sol transition in gellan gum aqueous solutions. *Carbohydrate Polymers, 30*, 109–119.

Mohammed, Z. H., Hember, M. W. N., Richardson, R. K., & Morris, E. R. (1998). Kinetic and equilibrium processes in the formation and melting of agarose gels. *Carbohydrate Polymers, 36*, 15–26.

Murphy, R. M. (1997). Static and dynamic light scattering of biological macromolecules: What can we learn? *Current Opinion in Biotechnology, 8*, 25–30.

Nanjawade, B. K., Manvi, F. V., & Manjappa, A. S. (2007). In situ-forming hydrogels for sustained ophthalmic drug delivery. *Journal of Controlled Release, 122*, 119–134.

Nisbet, D. R., Crompton, K. E., Hamilton, S. D., Shirakawa, S., Prankerd, R. J., Finkelstein, D. I., et al. (2006). Morphology and gelation of thermosensitive xyloglucan hydrogels. *Biophysical Chemistry, 121*, 14–20.

Norziah, M. H., Foo, S. L., & Karim, A. A. (2006). Rheological studies on mixtures of agar (*Gracilaria changii*) and [kappa]-carrageenan. *Food Hydrocolloids, 20*, 204–217.

Núñez-Santiago, M. C., & Tecante, A. (2007). Rheological and calorimetric study of the sol–gel transition of [kappa]-carrageenan. *Carbohydrate Polymers, 69*, 763–773.

Petrov, P., Rangelov, S., Novakov, C., Brown, W., Berlinova, I., & Tsvetanov, C. B. (2002). Core-corona nanoparticles formed by high molecular weight poly(ethylene oxide)–b-poly(alkylglycidyl ether) diblock copolymers. *Polymer, 43*, 6641–6651.

Picout, D. R., Ross-Murphy, S. B., Errington, N., & Harding, S. E. (2003). Pressure cell assisted solubilization of xyloglucans: Tamarind seed polysaccharide and detarium gum. *Biomacromolecules, 4*, 799–807.

Reiter, W. D. (2002). Biosynthesis and properties of the plant cell wall. *Current Opinion in Plant Biology, 5*, 536–542.

Ruan, D., Lue, A., & Zhang, L. (2008). Gelation behaviors of cellulose solution dissolved in aqueous NaOH/thiourea at low temperature. *Polymer, 49*, 1027–1036.

Schmaljohann, D. (2006). Thermo- and pH-responsive polymers in drug delivery. *Advanced Drug Delivery Reviews, 58*, 1655–1670.

Shirakawa, M., Yamatoya, K., & Nishinari, K. (1998). Tailoring of xyloglucan properties using an enzyme. *Food Hydrocolloids, 12*, 25–28.

Tecante, A., & Doublier, J. L. (1999). Steady flow and viscoelastic behavior of crosslinked waxy corn starch-[kappa]-carrageenan pastes and gels. *Carbohydrate Polymers, 40*, 221–231.

Urakawa, H., Mimura, M., & Kajuwara, K. (2002). Diversity and versatility of plant seed xyloglucan. *Trends in Glycoscience and Glucotechnology, 14*, 355–376.

Wang, Q., Rademacher, B., Sedlmeyer, F., & Kulozik, U. (2005). Gelation behaviour of aqueous solutions of different types of carrageenan investigated by low-intensity-ultrasound measurements and comparison to rheological measurements. *Innovative Food Science & Emerging Technologies, 6*, 465–472.

Weng, L., Zhang, L., Ruan, D., Shi, L., & Xu, J. (2004). Thermal gelation of cellulose in a NaOH/thiourea aqueous solution. *Langmuir, 20*, 2086–2093.

Yapeng Fang, K. N. (2004). Gelation behaviors of schizophyllan-sorbitol aqueous solutions. *Biopolymers, 73*, 44–60.

Zhang, Y., Xu, X., & Zhang, L. (2008). Dynamic viscoelastic behavior of triple helical Lentinan in water: Effect of temperature. *Carbohydrate Polymers, 73*, 26–34.